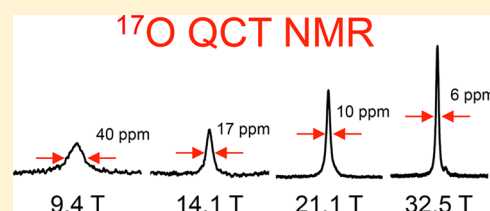


A Quadrupole-Central-Transition ^{17}O NMR Study of Nicotinamide: Experimental Evidence of Cross-Correlation between Second-Order Quadrupolar Interaction and Magnetic Shielding Anisotropy

Jiahui Shen,[†] Victor Terskikh,^{†,‡,§} Xiaoling Wang,[§] Ivan Hung,[§] Zhehong Gan,[§] and Gang Wu^{*,†,§}[†]Department of Chemistry, Queen's University, 90 Bader Lane, Kingston, Ontario, Canada K7L 3N6[‡]Department of Chemistry, University of Ottawa, Ottawa, Ontario, Canada K1N 6N5[§]National High Magnetic Field Laboratory, 1800 East Paul Dirac Drive, Tallahassee, Florida 32310, United States

Supporting Information

ABSTRACT: We have examined the ^{17}O quadrupole-central-transition (QCT) NMR signal from ^{17}O nicotinamide (vitamin B3) dissolved in glycerol. Measurements were performed at five magnetic fields ranging from 9.4 to 35.2 T between 243 and 363 K. We found that, in the ultraslow motion regime, cross-correlation between the second-order quadrupole interaction and magnetic shielding anisotropy is an important contributor to the transverse relaxation process for the ^{17}O QCT signal of ^{17}O nicotinamide. While such a cross-correlation effect has generally been predicted by relaxation theory, we report here the first experimental evidence for this phenomenon in solution-state NMR for quadrupolar nuclei. We have discussed the various factors that determine the ultimate resolution limit in QCT NMR spectroscopy. The present study also highlights the advantages of performing QCT NMR experiments at very high magnetic fields (e.g., 35.2 T).



1. INTRODUCTION

Quadrupole-central-transition (QCT) NMR spectroscopy for half-integer quadrupolar spins ($I > 1/2$) in isotropic liquids is based on the fact that, in the slow motion regime, the transverse relaxation rate constant (thus the line width) for the only detectable NMR signal (i.e., the QCT signal) is *inversely* proportional to both the molecular rotational correlation time (τ_C) and the Larmor frequency (ω_0) of the nucleus under study.^{1–8} As a result, it is possible to observe relatively narrow QCT NMR signals from otherwise hard to study quadrupolar nuclei for slowly tumbling molecules in solution.^{9–14} Indeed, several recent studies have utilized this idea in ^{17}O ($I = 5/2$) NMR studies of biological macromolecules in aqueous solution.^{15–17} Of course, this basic principle of QCT NMR spectroscopy is valid only when the first-order quadrupole interaction is the predominant relaxation mechanism. Recently, we discovered that, when the molecular motion is *ultraslow*, the first-order quadrupole relaxation mechanism diminishes for the QCT signal and the second-order quadrupole interaction becomes a dominant relaxation mechanism.¹⁸ Under such a circumstance, the transverse relaxation rate constant of a QCT signal is *proportional* to τ_C , thus making it undesirable to record QCT signals at exceedingly long τ_C values. However, since this second-order quadrupole contribution is still *inversely* proportional to ω_0^2 , recording QCT signals at very high magnetic fields would still be beneficial in reducing this relaxation contribution to the line width. The latest example is the remarkable line width reduction observed for the ^{17}O QCT signals from $[3,5,6-^{17}\text{O}_3]\text{-D-glucose}$ at 35.2 T.¹⁹ Unfortunately, many quadrupolar nuclei also experience considerable shielding

anisotropy (SA). Since the SA contribution to the transverse relaxation rate is proportional to ω_0^2 , QCT signals will be significantly broadened by the SA relaxation at very high magnetic fields. In practice, it is important to search for an optimal combination of τ_C and ω_0 , at which the QCT signal exhibits the narrowest line width. For small molecules, τ_C can be readily tuned over several orders of magnitude by a combination of the choice of solvent and sample temperature.¹⁸ For biological macromolecules in aqueous solution, however, the control of τ_C is relatively limited.¹⁶ Furthermore, the optimal condition also depends critically on the interplay of second-order quadrupole interaction and SA. In our previous study, the second-order quadrupole and SA relaxation mechanisms were treated independently.¹⁸ Some time ago, Werbelow²⁰ provided a theoretical analysis predicting that cross-correlation between the second-order quadrupole interaction and SA can be observable for QCT signals in the slow motion regime. However, to our knowledge, no experimental evidence has ever been reported in the literature for this phenomenon in solution-state QCT NMR studies. It is worth noting that cross-correlation between two tensorial properties is commonplace in solid-state NMR.²¹ A similar cross-correlation effect between the dipolar interaction and SA has long been utilized in solution-state NMR experiments for studying spin-1/2 nuclei (i.e., TROSY).^{22–26}

Received: March 12, 2018

Revised: April 19, 2018

Published: April 23, 2018

In this study, we set out to examine the possibility that cross-correlation between the second-order quadrupolar interaction and SA could be important for the ^{17}O QCT signal from [^{17}O]nicotinamide (vitamin B3). The reason for choosing [^{17}O]nicotinamide as a test system is because the carbonyl oxygen atom in the amide functional group is known to exhibit relatively large ^{17}O SA.^{27–29} In comparison, in our recent ^{17}O QCT NMR study of [^{17}O]glucose, for which the ^{17}O SA is rather small,³⁰ we did not observe any cross-relaxation effect.¹⁸

2. THEORY

It has been well established that, for half-integer quadrupolar nuclei, $I > 1/2$, the nuclear quadrupole transverse relaxation process generally contains $(I + 1/2)$ components, resulting in a multiexponential NMR signal. Under the slow motion limit ($\omega_0\tau_C > 1$), however, it is very often the case that only the CT signal is observable. If the first-order quadrupole interaction is the only relaxation mechanism, an approximate analytical expression was recently proposed to describe the transverse relaxation rate³¹

$$R_2^{\text{Q}} = \frac{1}{T_2^{\text{Q}}} = \frac{3}{80} \frac{2I + 3}{I^2(2I - 1)} \omega_{\text{Q}}^2 [J(\omega_0) + J(2\beta\omega_0)] \quad (1)$$

where ω_{Q} is the nuclear quadrupole coupling constant in angular frequency units ($\omega_{\text{Q}} = 2\pi C_{\text{Q}}$)

$$J(\omega_0) = \frac{\tau_C}{1 + (\omega_0\tau_C)^2} \quad (2)$$

and

$$\beta = \sqrt{\frac{2}{I(I + 1) - \frac{7}{4}}} \quad (3)$$

It is clear from eq 1 that the relaxation contribution to the CT from the first-order quadrupole interaction vanishes when $\omega_0\tau_C \gg 1$. Under such a circumstance, we showed recently that the second-order quadrupole interaction would become the predominant relaxation mechanism for the CT.¹⁸ The secular contribution of the CT transverse relaxation is determined by the anisotropic (orientation dependent) part of the second-order quadrupole interaction. Following Cohen and Reif,³² we can write the second-order quadrupole shift (in angular frequency units) from an axially symmetric tensor ($\eta_{\text{Q}} = 0$) under the static condition as

$$\omega_{\text{Q}}^{(2)}(\theta) = -\frac{9}{64} \frac{I(I + 1) - \frac{3}{4}}{I^2(2I - 1)^2} \left(\frac{\omega_{\text{Q}}^2}{\omega_0} \right) \left[-\frac{72}{35} P_4(\theta) + \frac{32}{21} P_2(\theta) + \frac{8}{15} \right] \quad (4)$$

where P_2 and P_4 are the second and fourth Legendre polynomials, respectively, and θ is the angle between the unique QC tensor component and the applied magnetic field. It is often the case that the CT also experiences an anisotropic chemical shift. Assuming the chemical shift tensor is also axially symmetric ($\eta_{\text{CS}} = 0$), the signal shift (in angular frequency) can be written as³³

$$\omega_{\text{CS}}(\theta) = \omega_0 \left[1 - \left(\sigma_{\text{iso}} + \frac{2}{3} \Delta\sigma_{\text{CS}} P_2(\theta') \right) \right] \quad (5)$$

where $\Delta\sigma_{\text{CS}} = \sigma_{\text{zz}} - (\sigma_{\text{xx}} + \sigma_{\text{yy}})/2 = \sigma_{\parallel} - \sigma_{\perp}$ and θ' is the angle between the unique CS tensor component and the magnetic field. Combining eqs 4 and 5, we obtain the total shift of the CT signal as

$$\omega_{\text{total}} = \omega_{\text{Q}}^{(2)}(\theta) + \omega_{\text{CS}}(\theta') \quad (6)$$

When the molecule of interest undergoes isotropic tumbling in solution, both θ and θ' become time dependent, resulting in a time-dependent signal shift, i.e., $\omega_{\text{total}}(t)$. This represents a fluctuation of the local magnetic field at the nucleus along the B_0 direction (the z -axis). Using the random field model,³⁴ we can evaluate the secular (or adiabatic) contribution of $\omega_{\text{total}}(t)$ to the CT transverse relaxation rate by computing the following autocorrelation function

$$R_2 = \int_0^{\infty} \langle \omega(t - \tau)\omega(t) \rangle d\tau \quad (7)$$

Using the following well-known correlation functions

$$\langle P_l(\theta(t - \tau))P_{l'}(\theta(t)) \rangle = \frac{\delta_{ll'}}{2l + 1} e^{-l(l+1)D_{\text{R}}\tau} \quad (8)$$

where l (or l') can be either 2 or 4 and $D_{\text{R}} = (6\tau_C)^{-1}$ is the diffusion constant in isotropic liquids, one can readily obtain the following results

$$R_2 = R_2^{\text{Q2}} + R_2^{\text{SA}} + R_2^{\text{Q2/SA}} \quad (9)$$

where the first two contributions are from the second-order quadrupole interaction (Q2) and SA, respectively, whereas the third term is the cross-correlation between them (Q2/SA). Their expressions are

$$R_2^{\text{Q2}} = \frac{298}{875} \left[\frac{3}{16} \frac{I(I + 1) - \frac{3}{4}}{I^2(2I - 1)^2} \right]^2 \left(\frac{\omega_{\text{Q}}^2}{\omega_0} \right)^2 \tau_C \quad (10)$$

$$R_2^{\text{SA}} = \frac{4}{45} (\omega_0 \Delta\sigma_{\text{CS}})^2 \tau_C \quad (11)$$

$$R_2^{\text{Q2/SA}} = \frac{2}{35} \frac{I(I + 1) - \frac{3}{4}}{I^2(2I - 1)^2} \omega_{\text{Q}}^2 \Delta\sigma_{\text{CS}} \left(\frac{3 \cos^2 \beta - 1}{2} \right) \tau_C \quad (12)$$

In eq 12, the term $(3 \cos^2 \beta - 1)/2$ stems from the transformation between the principal axis systems between the QC and CS tensors. The results of eqs 10–12 are fully consistent with those previously derived by Werbelow.²⁰ It is important to further comment on the Q2/SA cross-correlation term as expressed in eq 12. First, the Q2/SA term is independent of the magnetic field. Second, since both $\Delta\sigma_{\text{CS}}$ and $(3 \cos^2 \beta - 1)/2$ can be either positive or negative, the sign of the Q2/SA term can be either positive or negative. The consequence is that the Q2/SA term can be of either benefit or nuisance in terms of the line width of a QCT signal, depending on the intrinsic tensor interplay in a particular functional group. We should also note that, in the above derivations of eqs 9–12, QC and CS tensors were assumed to be axially symmetric. For general cases, eqs 9–12 can be modified simply by replacing C_{Q} and $\Delta\sigma_{\text{CS}}$ by $P_{\text{Q}} = C_{\text{Q}}(1 + \eta_{\text{Q}}^2)^{1/2}$ and $P_{\text{SA}} = \Delta\sigma_{\text{CS}}(1 + \eta_{\text{CS}}^2)^{1/2}$, respectively, as well as the geometric factor $(3 \cos^2 \beta - 1)/2$ by the following expression:

$$\left. \begin{aligned} & \frac{1}{2} \left\{ 3 \cos^2 \beta - 1 + \sin^2 \beta (\eta_{\text{CS}} \cos 2\alpha + \eta_{\text{Q}} \cos 2\gamma) \right. \\ & + \frac{\eta_{\text{CS}} \eta_{\text{Q}}}{3} [(\cos^2 \beta + 1) \cos 2\alpha \cos 2\gamma \\ & \left. - 2 \cos \beta \sin 2\alpha \sin 2\gamma] \right\} \end{aligned} \right\} \quad (13)$$

3. EXPERIMENTAL SECTION

[^{17}O]Nicotinamide was prepared by following a literature procedure.³⁵ The ^{17}O enrichment level in [^{17}O]nicotinamide was estimated by solution ^{17}O NMR to be about 10%. The solution sample used for ^{17}O QCT experiments was prepared by dissolving 74 mg of [^{17}O]nicotinamide in 0.567 g of neat glycerol. ^{17}O QCT signals were recorded at five magnetic fields, 9.4, 11.7, 14.1, 21.1, and 35.2 T. The experiments at 35.2 T were performed with the series-connected hybrid (SCH) magnet at NHMFL.¹⁹ The ^{13}C spin–lattice relaxation times (T_1) were determined by the inversion–recovery method for nicotinamide dissolved in glycerol at 11.7 T over a temperature range between 278 and 388 K. Static ^{17}O NMR spectra were acquired for a solid sample of [^{17}O]nicotinamide at 14.1 and 21.1 T. ^{17}O MAS spectra were recorded at 21.1 T with a Bruker 2.5 mm HX MAS probe. All ^{17}O chemical shifts were referenced to an external sample of $\text{H}_2\text{O}(\text{liq})$. Spectral simulations were performed with DMFit.³⁶

4. RESULTS AND DISCUSSION

4.1. The Hydrodynamic Model. As a first step of our investigation, it is necessary to determine a hydrodynamic model for properly describing molecular tumbling of nicotinamide in glycerol. The general Stokes–Einstein–Debye (SED) model is based on

$$\tau_{\text{C}} = \frac{V_{\text{h}} \eta}{kT} \quad (14)$$

where V_{h} is the hydrodynamic volume of the solute molecule, η is the viscosity of the solvent, k is the Boltzmann constant, and T is the absolute temperature. This model is valid when the size of the solute molecule is much larger than the solvent molecule, i.e., the so-called “stick” limit. In the case of nicotinamide dissolved in glycerol, because the sizes of solute and solvent molecules are comparable, the SED model of eq 14 can be extended to the following Gierer–Wirtz model³⁷

$$\tau_{\text{C}} = \frac{fV_{\text{h}} \eta}{kT} \quad (15)$$

where

$$f = \frac{1}{6(a_{\text{s}}/a) + (1 + a_{\text{s}}/a)^{-3}} \quad (16)$$

In the above equation, a_{s} and a are the hydrodynamic radii of the solvent and solute molecules, respectively. The Gierer–Wirtz model can properly describe the rotational dynamics for cases where solute and solvent molecules are of similar sizes (the slip limit). For example, when $a_{\text{s}} = a$, $f = 0.16$. This means that the “effective” hydrodynamic volume in the slip limit is considerably smaller than V_{h} . For glycerol, the temperature dependence of its viscosity, η , has been well established³⁸ and used in our previous study of D-glucose dissolved in glycerol.¹⁸

To test this hydrodynamic model (eqs 15 and 16), we measured the ^{13}C spin–lattice relaxation time (T_1) for nicotinamide dissolved in glycerol. The measurements were carried out at 11.7 T over a temperature range between 278 and 388 K (data are listed in the Supporting Information). Figure 1

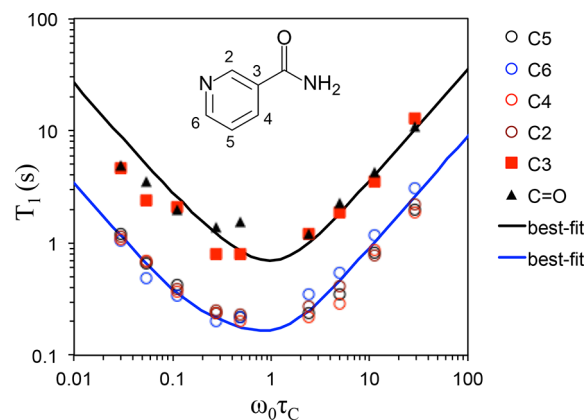


Figure 1. Experimental (symbols) and calculated (blue and black traces) ^{13}C T_1 data measured at 11.7 T for nicotinamide dissolved in glycerol. The atomic numbering is shown in the inset.

shows the experimental T_1 data for all ^{13}C nuclei from nicotinamide dissolved in glycerol. For ^{13}C nuclei, the main relaxation mechanisms are the ^1H – ^{13}C dipole–dipole and ^{13}C shielding anisotropy (SA) and their contributions to T_1 are well-known³⁹

$$\left(\frac{1}{T_1} \right)_{\text{total}} = \left(\frac{1}{T_1} \right)_{\text{DD}} + \left(\frac{1}{T_1} \right)_{\text{SA}} \quad (17)$$

where

$$\begin{aligned} \left(\frac{1}{T_1} \right)_{\text{DD}} &= \frac{N_{\text{H}}}{20} (2\pi R_{\text{DD}})^2 [J(\omega_{\text{H}} - \omega_{\text{C}}) + 3J(\omega_{\text{C}}) \\ &+ 6J(\omega_{\text{H}} + \omega_{\text{C}})] \end{aligned} \quad (18)$$

$$\left(\frac{1}{T_1} \right)_{\text{SA}} = \frac{1}{15} (\omega_{\text{C}} P_{\text{SA}})^2 J(\omega_{\text{C}}) \quad (19)$$

When we initially applied eqs 15–19 to fit the ^{13}C T_1 data shown in Figure 1, we found that only the T_1 data recorded at high temperatures (>308 K) can be properly fitted with the following parameters: $fV_{\text{h}} = 17 \times 10^{-30} \text{ m}^3$, $P_{\text{SA}} = 140$ (C2, C4, C5, C6) and 155 (C3, C=O) ppm, $R_{\text{DD}} = 23.316$ kHz (for a C–H bond length of 1.09 Å), and long-range $R_{\text{DD}} = 3.8$ kHz (for C3 and C=O). On the basis of the crystal structure of nicotinamide,⁴⁰ V_{h} can be estimated to be $144 \times 10^{-30} \text{ m}^3$; therefore, $f = 0.12$ for nicotinamide dissolved in glycerol. This f value is in good agreement with the prediction from eq 16. The P_{SA} values listed above are also consistent with the known ^{13}C CS tensors for similar molecules.⁴¹ Further examination of the low-temperature (<308 K) T_1 data suggests an effective hydrodynamic volume of greater than $17 \times 10^{-30} \text{ m}^3$. This can be explained by the tendency of nicotinamide molecules to self-associate most likely through hydrogen bonding at low temperatures.⁴² Indeed, the ^1H NMR spectra of nicotinamide show that the signals from the amino protons display a high-frequency shift as the sample temperature is decreased (data are shown in the Supporting Information), which is indicative of

hydrogen bond formation. Therefore, we introduced a simple “two-size model” to simultaneously fit the experimental ^{13}C T_1 data for the entire temperature range. For $T < 308$ K, we used $fV_h = 45 \times 10^{-30} \text{ m}^3$. As seen from Figure 1, this model produces a satisfactory fit of the experimental ^{13}C T_1 data. As will be shown in the next section, this hydrodynamic model also works well for ^{17}O NMR data.

4.2. ^{17}O NMR Results. Now that we have established a suitable hydrodynamic model for describing nicotinamide tumbling in glycerol, we turn our attention to ^{17}O NMR results. First, let us examine the ^{17}O NMR signal of [^{17}O]nicotinamide at 11.7 T in both the fast ($\omega_0\tau_C < 1$) and slow ($\omega_0\tau_C > 1$) motion regimes. As seen from Figure 2, in the

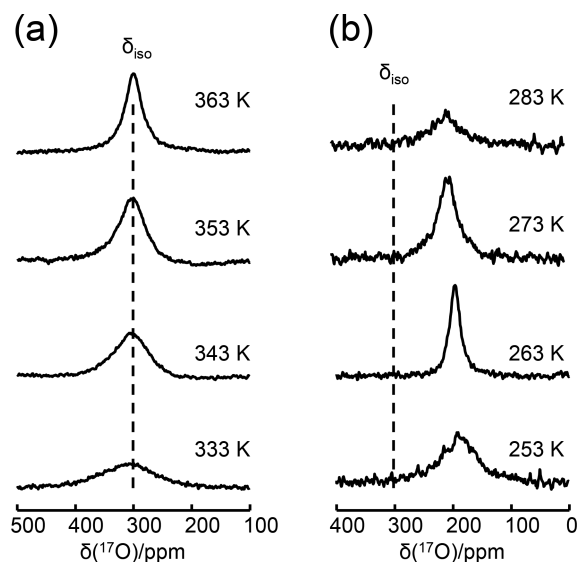


Figure 2. Experimental ^{17}O NMR spectra of [^{17}O]nicotinamide dissolved in glycerol at 11.7 T in the fast (a) and slow (b) motion regimes.

fast motion regime, the observed ^{17}O NMR signal originates from all degenerate transitions and appears at the true chemical shift position, $\delta_{\text{iso}} = 303$ ppm. The line width of this ^{17}O NMR signal decreases when the temperature of the sample is increased. In comparison, in the slow motion regime, the only observable ^{17}O NMR signal is the so-called QCT signal.

The position of the QCT signal (in the present case, 200 ppm) is known to be significantly shifted from δ_{iso} to a lower frequency due to the so-called dynamic frequency shift.⁴ The dynamic frequency shift is proportional to $(\omega_0)^{-2}$, as will be discussed in detail in a later section. More importantly, as seen from Figure 2, the line width of the ^{17}O QCT signal initially decreases as the temperature is lowered (< 283 K), reaches a minimum (at 263 K), and then increases with the further decrease of the sample temperature (< 263 K). As a result, it is possible to observe a relatively narrow ^{17}O QCT signal at certain low temperatures. For example, at 263 K, the full width at half-height (fwhh) of the ^{17}O QCT signal for [^{17}O]nicotinamide is about 1800 Hz (26 ppm), which is smaller than that observed at 363 K, 2450 Hz (36 ppm).

To fully understand the various factors that determine the QCT line width, we recorded the ^{17}O QCT signal for [^{17}O]nicotinamide at five different magnetic fields ranging from 9.4 to 35.2 T. As seen from Figure 3, while the ^{17}O QCT signal displays similar temperature dependences at various magnetic fields, the minimal line width (in ppm) decreases drastically with the increase of the applied magnetic field. For example, the fwhh is decreased from 41 ppm (2200 Hz) observed at 9.4 T to only 6 ppm (1250 Hz) at 35.2 T. This general behavior is similar to what we previously reported for [^{17}O]-D-glucose.^{18,19} All of these results demonstrate the tremendous gains in both sensitivity and resolution by carrying out ^{17}O QCT NMR experiments at very high magnetic fields (e.g., 35.2 T). As demonstrated in previous studies,^{15–18} from the field-dependent positions of the ^{17}O QCT signal, as shown in Figure 4, one can obtain the following ^{17}O NMR parameters for [^{17}O]nicotinamide: $P_Q = 8.7 \pm 0.5$ MHz and $\delta_{\text{iso}} = 302 \pm 2$ ppm.

Figure 5a displays all of the ^{17}O line width data (in ppm) obtained for [^{17}O]nicotinamide. There are two reasons that the line width data are expressed in units of ppm rather than Hz. First, this is a better measure of describing the resolving power as a function of the applied magnetic field. Second, this allows better separation of data for visual inspection. Using the hydrodynamic model established from the ^{13}C T_1 data as explained earlier, we were able to fit all of the ^{17}O NMR line width data shown in Figure 5a using eqs 9–12 and the following ^{17}O NMR parameters for [^{17}O]nicotinamide: $P_Q = 9.0 \pm 0.2$ MHz and $P_{\text{SA}} = -620 \pm 50$ ppm. Here we used $\beta =$

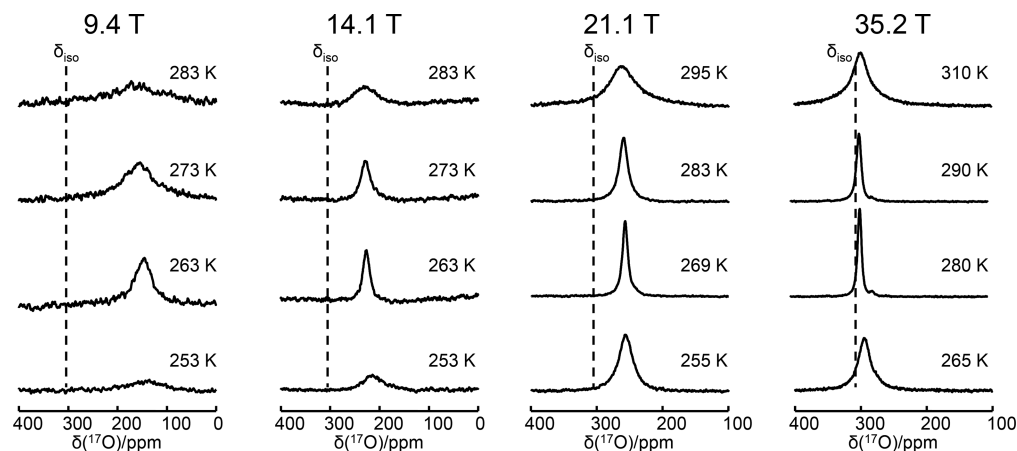


Figure 3. Experimental ^{17}O QCT NMR signals of [^{17}O]nicotinamide dissolved in glycerol. The magnetic field strength is shown at the top of each panel.

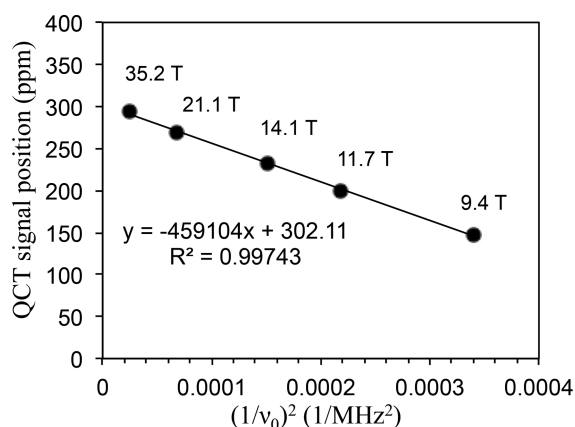


Figure 4. Dependence of the ^{17}O QCT signal position observed for ^{17}O nicotinamide dissolved in glycerol on the applied magnetic field. In each case, the ^{17}O QCT signal was referenced to an external sample of $\text{H}_2\text{O}(\text{liq})$.

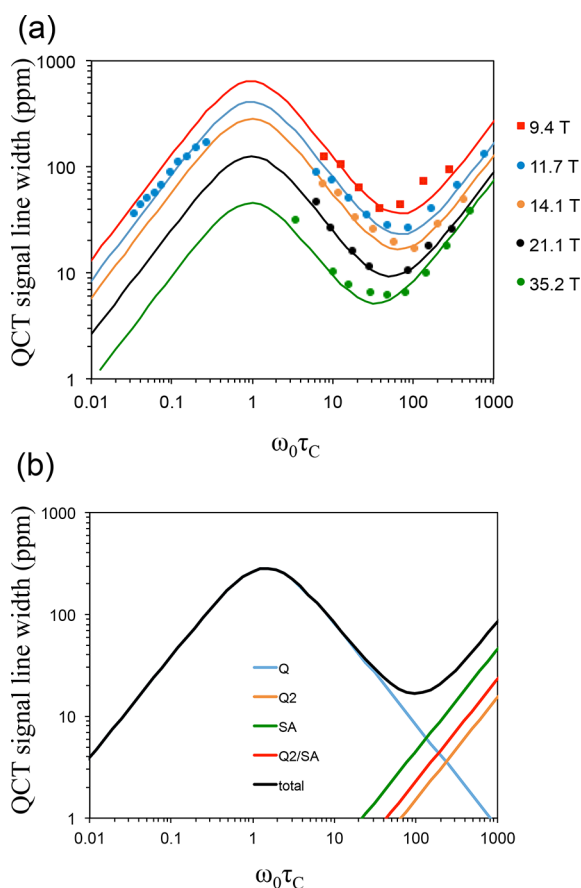


Figure 5. (a) Line width (in ppm) of the ^{17}O QCT signal observed for ^{17}O nicotinamide dissolved in glycerol as a function of $\omega_0\tau_C$. (b) Illustration of individual relaxation mechanisms for ^{17}O nicotinamide at 14.1 T.

90° or $(3 \cos^2 \beta - 1)/2 = -0.5$ on the basis of previous solid-state ^{17}O NMR studies of amides.^{27–29} Figure 5b illustrates how the four individual relaxation contributions (Q, Q2, SA, and Q2/SA) change over the entire motional range for nicotinamide. In the fast motion region ($\omega_0\tau_C < 1$), Q is the predominant relaxation mechanism. In the slow motion regime ($\omega_0\tau_C > 1$), while the contribution from Q gradually diminishes as $\omega_0\tau_C$ increases, Q2, SA, and Q2/SA become increasingly

important at high $\omega_0\tau_C$ values. For example, at close to the minimal line width ($\omega_0\tau_C \approx 100$), the individual contributions are Q (35%), SA (35%), Q2/SA (18%), and Q2 (12%). The situation is very different at $\omega_0\tau_C \approx 1000$, where the individual contributions are Q (1%), SA (54%), Q2/SA (27%), and Q2 (18%). Clearly, in all of these cases, the contribution from the cross-correlation term Q2/SA cannot be ignored.

To further confirm the ^{17}O NMR tensor parameters extracted from the above analysis, we recorded solid-state ^{17}O NMR spectra for ^{17}O nicotinamide at 14.1 and 21.1 T. Figure 6 shows the ^{17}O MAS and static NMR spectra at 21.1 T.

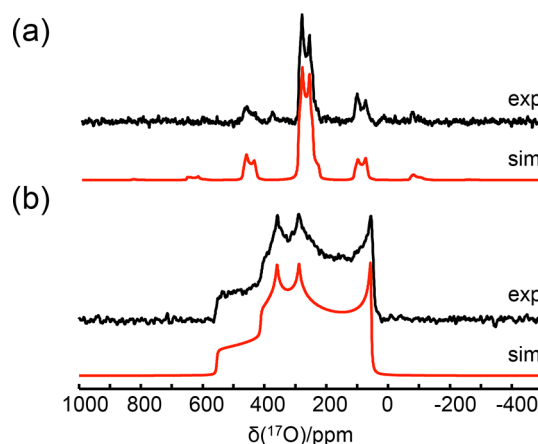


Figure 6. Experimental (black trace) and simulated (red trace) 22 kHz MAS (a) and static (b) ^{17}O NMR spectra of a solid sample of ^{17}O nicotinamide. Both spectra were recorded at 21.1 T.

Following a well-established procedure for spectral fitting,²⁷ we obtained both the QC and CS tensors and their relative orientation: $C_Q(^{17}\text{O}) = 8.5 \pm 0.2$ MHz and $\eta_Q = 0.3 \pm 0.1$; $\delta_{\text{iso}}(^{17}\text{O}) = 305 \pm 2$ ppm, $\delta_{11} = 523 \pm 10$, $\delta_{22} = 403 \pm 10$, $\delta_{33} = -11 \pm 10$ ppm; $\alpha = 73 \pm 5$, $\beta = 90 \pm 2$, $\gamma = 90 \pm 2^\circ$. These parameters give $P_Q = 8.6 \pm 0.2$ MHz and $P_{\text{SA}} = -485 \pm 20$ ppm. We should point out that, while these values appear to be somewhat smaller than those obtained from the QCT signal analysis described earlier, the small reductions in both P_Q (4%) and P_{SA} (22%) can be attributed to the strong hydrogen bonding effects present in solids.^{43–45}

Now in order to have a better understanding of the condition under which the cross-correlation term Q2/SA may become important, we use ^{17}O QCT NMR as an example to evaluate individual contributors (Q, Q2, SA, and Q2/SA) in two typical cases: case 1, $P_Q = 9$ MHz and $P_{\text{SA}} = 600$ ppm; case 2, $P_Q = 10$ MHz and $P_{\text{SA}} = 50$ ppm. The first case is typical of what is seen from a general carbonyl compound, and the second case resembles those from hydroxyl groups in carbohydrate molecules (e.g., glucose). Here we are particularly interested in the magnetic field dependence. The line width for a QCT signal can be calculated from eqs 1–3 and 9–12. Because the situation also depends on τ_C , we performed line width calculations using two typical τ_C values for relatively slow molecular tumbling motion: $\tau_C = 5 \times 10^{-8}$ and 5×10^{-7} s. As seen from Figure 7a, when $\tau_C = 5 \times 10^{-8}$ s in case 1, the most important contributors to the line width are Q and SA. At $\tau_C = 5 \times 10^{-7}$ s, the value of $\omega_0\tau_C$ increases from 16 to 78 when $\nu_0(^{17}\text{O})$ is changed from 50 to 250 MHz. In this case, because Q and SA display opposite field dependences, the line width exhibits a minimal point as a function of $\nu_0(^{17}\text{O})$. In

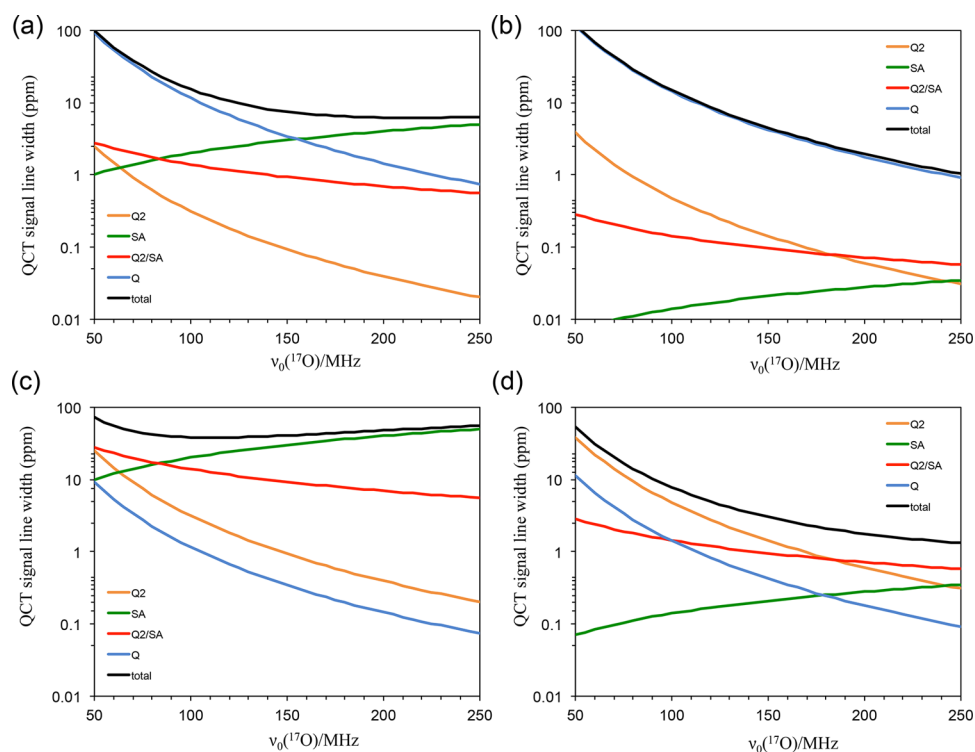


Figure 7. Theoretical line width (in ppm) of a ^{17}O QCT signal as a function of the ^{17}O Larmor frequency. (a) $P_Q = 9$ MHz, $P_{SA} = 600$ ppm, $\tau_C = 5 \times 10^{-8}$ s. (b) $P_Q = 10$ MHz, $P_{SA} = 50$ ppm, $\tau_C = 5 \times 10^{-8}$ s. (c) $P_Q = 9$ MHz, $P_{SA} = 600$ ppm, $\tau_C = 5 \times 10^{-7}$ s. (d) $P_Q = 10$ MHz, $P_{SA} = 50$ ppm, $\tau_C = 5 \times 10^{-7}$ s.

comparison, for case 2 at $\tau_C = 5 \times 10^{-8}$ s, Q is the predominant factor and its contribution to the line width decreases monotonically with the increase of $\nu_0(^{17}\text{O})$, as seen in Figure 7b. At $\tau_C = 5 \times 10^{-7}$ s, the value of $\omega_0\tau_C$ is between 160 and 780, which can be considered to be in the ultraslow motion regime. Now in case 1, SA and Q2/SA are predominant factors; see Figure 7c. In case 2, however, Q2 and Q2/SA are the most important for the most part, i.e., $\nu_0(^{17}\text{O}) > 100$ MHz, as seen from Figure 7d. One general conclusion drawn from the data shown in Figure 7 is that the resolution limit in ^{17}O QCT NMR can be greatly improved by utilizing ultrahigh magnetic fields for case 2 but not so much for case 1.

5. CONCLUSIONS

We have observed the ^{17}O NMR signal from $[^{17}\text{O}]$ nicotinamide dissolved in glycerol over a large range of motion where the molecular rotational correlation time changes more than 4 orders of magnitude. A simple “two-size” hydrodynamic model was developed on the basis of the ^{13}C T_1 data measured for nicotinamide between 278 and 388 K. This hydrodynamic model was then used to interpret the ^{17}O QCT NMR results obtained at five magnetic fields ranging from 9.4 to 35.2 T. We demonstrate that the Q2/SA cross-correlation term is an important contributor to the total line width of the ^{17}O QCT signal for nicotinamide. Now we have a complete understanding of the four components of the quadrupolar relaxation mechanism: Q, Q2, SA, and Q2/SA. We have also applied the theoretical expressions developed in this study to some typical cases encountered in ^{17}O QCT NMR and discussed the resolution limit achievable with QCT NMR spectroscopy for slowly tumbling macromolecules. The results reported in this study show that the advent of very high magnetic fields (e.g.,

35.2 T) brings significant benefits in both sensitivity and resolution of ^{17}O QCT NMR spectroscopy.

■ ASSOCIATED CONTENT

Supporting Information

The Supporting Information is available free of charge on the ACS Publications website at DOI: 10.1021/acs.jpcb.8b02417.

Experimental ^{13}C T_1 results and ^1H NMR signal positions for nicotinamide dissolved in glycerol at different temperatures (PDF)

■ AUTHOR INFORMATION

Corresponding Author

*E-mail: wugang@queensu.ca.

ORCID

Victor Terskikh: 0000-0003-1514-2610

Gang Wu: 0000-0002-0936-9432

Notes

The authors declare no competing financial interest.

■ ACKNOWLEDGMENTS

G.W. thanks the Natural Sciences and Engineering Research Council (NSERC) of Canada for a discovery grant (Grant No. 23308-11). Access to the 900 MHz NMR spectrometer was provided by the National Ultrahigh-Field NMR Facility for Solids (Ottawa, Canada), a national research facility funded by the Canada Foundation for Innovation, the Ontario Innovation Trust, Recherche Québec, the National Research Council Canada, and Bruker BioSpin and managed by the University of Ottawa (<http://nmr900.ca>). NSERC is acknowledged for a Major Resources Support grant. This work was also supported by the National High Magnetic Field Laboratory through NSF

DMR-1157490 and the State of Florida and by a grant from NIH (P41 GM122698). We thank Dr. Xianqi Kong and Catherine Franey for assistance in synthesizing [¹⁷O] nicotinamide.

REFERENCES

- (1) Hubbard, P. S. Nonexponential Nuclear Magnetic Resonance Relaxation by Quadrupolar Interactions. *J. Chem. Phys.* **1970**, *53*, 985–987.
- (2) Bull, T. E. Nuclear Magnetic Relaxation of Spin-3/2 Nuclei Involved in Chemical Exchange. *J. Magn. Reson.* **1972**, *8*, 344–353.
- (3) Baram, A.; Luz, Z.; Alexander, S. Resonance Line Shapes for Semi-Integer Spins in Liquids. *J. Chem. Phys.* **1973**, *58*, 4558–4564.
- (4) Werbelow, L. G. NMR Dynamic Frequency Shifts and the Quadrupolar Interaction. *J. Chem. Phys.* **1979**, *70*, 5381–5383.
- (5) Bull, T. E.; Forsen, S.; Turner, D. L. Nuclear Magnetic Relaxation of Spin 5/2 and Spin 7/2 Nuclei Including the Effects of Chemical Exchange. *J. Chem. Phys.* **1979**, *70*, 3106–3111.
- (6) Werbelow, L.; Pouzard, G. Quadrupolar Relaxation. The Multiquantum Coherences. *J. Phys. Chem.* **1981**, *85*, 3887–3891.
- (7) Westlund, P. O.; Wennerström, H. NMR Lineshapes of I = 5/2 and I = 7/2 Nuclei. Chemical Exchange Effects and Dynamic Shifts. *J. Magn. Reson.* **1982**, *50*, 451–466.
- (8) Zhu, J.; Ye, E.; Tersikh, V.; Wu, G. Experimental Verification of the Theory of Nuclear Quadrupole Relaxation in Liquids over the Entire Range of Molecular Tumbling Motion. *J. Phys. Chem. Lett.* **2011**, *2*, 1020–1023.
- (9) Andersson, T.; Drakenberg, T.; Forsen, S.; Thulin, E.; Swaerd, M. Direct Observation of the ⁴³Ca NMR Signals from Ca²⁺ Ions Bound to Proteins. *J. Am. Chem. Soc.* **1982**, *104*, 576–580.
- (10) Butler, A.; Eckert, H.; Danzitz, M. J. ⁵¹V NMR as a Probe of Metal Ion Binding in Metalloproteins. *J. Am. Chem. Soc.* **1987**, *109*, 1864–1865.
- (11) Butler, A.; Eckert, H. ⁵¹V NMR as a Probe of Vanadium(V) Coordination to Human Apotransferrin. *J. Am. Chem. Soc.* **1989**, *111*, 2802–2809.
- (12) Aramini, J. M.; Vogel, H. J. Aluminum-27 and Carbon-13 NMR Studies of Aluminum(3+) Binding to Ovotransferrin and Its Half-Molecules. *J. Am. Chem. Soc.* **1993**, *115*, 245–252.
- (13) Aramini, J. M.; Germann, M. W.; Vogel, H. J. Field-Dependent Aluminum-27 NMR Studies of the Transferrins: An Approach for the Study of Metal Ion Binding Sites in Larger Proteins. *J. Am. Chem. Soc.* **1993**, *115*, 9750–9753.
- (14) Germann, M. W.; Aramini, J. M.; Vogel, H. J. Quadrupolar Metal Ion NMR Study of Ovotransferrin at 17.6 T. *J. Am. Chem. Soc.* **1994**, *116*, 6971–6972.
- (15) Zhu, J.; Kwan, I. C. M.; Wu, G. Quadrupole-Central-Transition ¹⁷O NMR Spectroscopy of Protein-Ligand Complexes in Solution. *J. Am. Chem. Soc.* **2009**, *131*, 14206–14207.
- (16) Zhu, J.; Wu, G. Quadrupole Central Transition ¹⁷O NMR Spectroscopy of Biological Macromolecules in Aqueous Solution. *J. Am. Chem. Soc.* **2011**, *133*, 920–932.
- (17) Young, R. P.; Caulkins, B. G.; Borchardt, D.; Bulloch, D. N.; Larive, C. K.; Dunn, M. F.; Mueller, L. J. Solution-State ¹⁷O Quadrupole Central-Transition NMR Spectroscopy in the Active Site of Tryptophan Synthase. *Angew. Chem., Int. Ed.* **2016**, *55*, 1350–1354.
- (18) Shen, J.; Tersikh, V.; Wu, G. Observation of the Second-Order Quadrupolar Interaction as a Dominant NMR Relaxation Mechanism in Liquids: The Ultraslow Regime of Motion. *J. Phys. Chem. Lett.* **2016**, *7*, 3412–3418.
- (19) Gan, Z.; Hung, I.; Wang, X.; Paulino, J.; Wu, G.; Litvak, I. M.; Gor'kov, P. L.; Brey, W. W.; Lendi, P.; Schiano, J. L.; Bird, M.; Dixon, I.; Toth, J.; Boebinger, G. S.; Cross, T. A. NMR Spectroscopy up to 35.2 T Using a Series-Connected Hybrid Magnet. *J. Magn. Reson.* **2017**, *284*, 125–136.
- (20) Werbelow, L. Adiabatic Nuclear Magnetic Resonance Linewidth Contributions for Central Transitions of I > 1/2 Nuclei. *J. Chem. Phys.* **1996**, *104*, 3457–3462.
- (21) Bryce, D. L.; Wasylishen, R. E. Quadrupolar Nuclei in Solids: Influence of Different Interactions on Spectra. In *NMR of Quadrupolar Nuclei in Solid Materials*; Wasylishen, R. E., Ashbrook, S. E., Wimperis, S., Eds.; John Wiley & Sons Ltd.: Chichester, U.K., 2012; Chapter 4.
- (22) Pervushin, K.; Riek, R.; Wider, G.; Wuthrich, K. Attenuated T₂ Relaxation by Mutual Cancellation of Dipole–Dipole Coupling and Chemical Shift Anisotropy Indicates an Avenue to NMR Structures of Very Large Biological Macromolecules in Solution. *Proc. Natl. Acad. Sci. U. S. A.* **1997**, *94*, 12366–12371.
- (23) Fernandez, C.; Wider, G. TROSY in NMR Studies of the Structure and Function of Large Biological Macromolecules. *Curr. Opin. Struct. Biol.* **2003**, *13*, 570–580.
- (24) Tugarinov, V.; Hwang, P.; Ollerenshaw, J. E.; Kay, L. E. Cross-Correlated Relaxation Enhanced ¹H–¹³C NMR Spectroscopy of Methyl Groups in Very High Molecular Weight Proteins and Protein Complexes. *J. Am. Chem. Soc.* **2003**, *125*, 10420–10428.
- (25) Ollerenshaw, J. E.; Tugarinov, V.; Kay, L. E. Methyl TROSY: Explanation and Experimental Verification. *Magn. Reson. Chem.* **2003**, *41*, 843–852.
- (26) Tugarinov, V.; Sprangers, R.; Kay, L. E. Line Narrowing in Methyl-TROSY Using Zero-Quantum ¹H–¹³C NMR Spectroscopy. *J. Am. Chem. Soc.* **2004**, *126*, 4921–4925.
- (27) Yamada, K.; Dong, S.; Wu, G. Solid-State ¹⁷O NMR Investigation of the Carbonyl Oxygen Electric-Field-Gradient Tensor and Chemical Shielding Tensor in Amides. *J. Am. Chem. Soc.* **2000**, *122*, 11602–11609.
- (28) Chekmenev, E. Y.; Waddell, K. W.; Hu, J.; Gan, Z.; Wittebort, R. J.; Cross, T. A. Ion-Binding Study by ¹⁷O Solid-State NMR Spectroscopy in the Model Peptide Gly-Gly-Gly at 19.6 T. *J. Am. Chem. Soc.* **2006**, *128*, 9849–9855.
- (29) Wu, G. Solid-State ¹⁷O NMR Studies of Organic and Biological Molecules. *Prog. Nucl. Magn. Reson. Spectrosc.* **2008**, *52*, 118–169.
- (30) Sefzik, T. H.; Houseknecht, J. B.; Clark, T. M.; Prasad, S.; Lowary, T. L.; Gan, Z.; Grandinetti, P. J. Solid-State ¹⁷O NMR in Carbohydrates. *Chem. Phys. Lett.* **2007**, *434*, 312–315.
- (31) Wu, G. An Approximate Analytical Expression for the Nuclear Quadrupole Transverse Relaxation Rate of Half-Integer Spins in Liquids. *J. Magn. Reson.* **2016**, *269*, 176–178.
- (32) Cohen, M. H.; Reif, F. Quadrupole Effects in Nuclear Magnetic Resonance Studies of Solids. In *Solid State Physics*; Seitz, F., Turnbull, D., Eds.; Academic Press Inc.: New York, 1957; Vol. 5, pp 321–438.
- (33) Abragam, A. *The Principles of Nuclear Magnetism*; Oxford University Press: London, 1961.
- (34) Levitt, M. H. *Spin Dynamics: Basics of Nuclear Magnetic Resonance*; John Wiley & Sons, Ltd.: Chichester, U.K., 2001.
- (35) Kolodziejaska-Huben, M.; Kaminski, Z.; Paneth, P. Preparation of ¹⁸O-Labelled Nicotinamide. *J. Labelled Compd. Radiopharm.* **2002**, *45*, 1005–1010.
- (36) Massiot, D.; Fayon, F.; Capron, M.; King, I.; Le Calve, S.; Alonso, B.; Durand, J.-O.; Bujoli, B.; Gan, Z.; Hoatson, G. Modelling One- and Two-Dimensional Solid-State NMR Spectra. *Magn. Reson. Chem.* **2002**, *40*, 70–76.
- (37) Gierer, A.; Wirtz, K. Molekulare Theorie der Mikrorreibung. *Z. Naturforsch., A: Phys. Sci.* **1953**, *8*, 532–538.
- (38) Trejo Gonzalez, J. A.; Longinotti, M. P.; Corti, H. R. The Viscosity of Glycerol–Water Mixtures Including the Supercooled Region. *J. Chem. Eng. Data* **2011**, *56*, 1397–1406.
- (39) Spiess, H. W. Rotation of Molecules and Nuclear Spin Relaxation. In *NMR Principles and Progress*; Diehl, P., Fluck, E., Kosfeld, R., Eds.; Springer-Verlag: Berlin, 1978; Vol. 15, pp 55–214.
- (40) Wright, W. B.; King, G. S. D. The Crystal Structure of Nicotinamide. *Acta Crystallogr.* **1954**, *7*, 283–288.
- (41) Duncan, T. M. *Chemical Shift Tensors*; The Farragut Press: Madison, WI, 1997.

(42) Coffman, R. E.; Kildsig, D. O. Self-Association of Nicotinamide in Aqueous Solution: Light-Scattering and Vapor Pressure Osmometry Studies. *J. Pharm. Sci.* **1996**, *85*, 848–853.

(43) Dong, S.; Ida, R.; Wu, G. A Combined Experimental and Theoretical ^{17}O NMR Study of Crystalline Urea: An Example of Large Hydrogen-Bonding Effects. *J. Phys. Chem. A* **2000**, *104*, 11194–11202.

(44) Wu, G.; Dong, S.; Ida, R.; Reen, N. A Solid-State ^{17}O Nuclear Magnetic Resonance Study of Nucleic Acid Bases. *J. Am. Chem. Soc.* **2002**, *124*, 1768–1777.

(45) Kong, X.; Brinkmann, A.; Terskikh, V.; Wasylishen, R. E.; Bernard, G. M.; Duan, Z.; Wu, Q.; Wu, G. Proton Probability Distribution in the $\text{O}\cdots\text{H}\cdots\text{O}$ Low-Barrier Hydrogen Bond: A Combined Solid-State NMR and Quantum Chemical Computational Study of Dibenzoylmethane and Curcumin. *J. Phys. Chem. B* **2016**, *120*, 11692–11704.